

- 1
2
3 2006;220(2):135–143.
4
5
6 16. Brizuela M, Garcia-Luis A, Viviente JL, Braceras I, Onate JI. Tribological study of lubricious
7
8 DLC biocompatible coatings. *J Mater Sci Mater Med* 2002;13(12):1129–1133.
9
10
11
12 17. Gutmanas EY, Gotman I. PIRAC Ti nitride coated Ti-6Al-4V head against UHMWPE
13
14 acetabular cup-hip wear simulator study. *J Mater Sci Mater Med* 2004;15(4):327–330.
15
16
17
18 18. Oka M, Ushio K, Kumar P, Ikeuchi K, Hyon SH, Nakamura T, Fujita H. Development of
19
20 artificial articular cartilage. *Proc Inst Mech Eng [H]* 2000;214(1):59–68.
21
22
23
24 19. Moro T, Takatori Y, Ishihara K, Konno T, Takigawa Y, Matsushita T, Chung UI, Nakamura K,
25
26 Kawaguchi H. Surface grafting of artificial joints with a biocompatible polymer for preventing
27
28 periprosthetic osteolysis. *Nature Mater* 2004;3:829–837.
29
30
31
32
33 20. Moro T, Takatori Y, Ishihara K, Nakamura K, Kawaguchi H. 2006 Frank Stinchfield Award:
34
35 Grafting of Biocompatible Polymer for Longevity of Artificial Hip Joints. *Clin Orthop Relat*
36
37 *Res* 2006;453:58–63.
38
39
40
41
42
43
44 21. Kyomoto M, Moro T, Konno T, Takadama H, Kawaguchi H, Takatori Y, Nakamura K,
45
46 Yamawaki N, Ishihara K. Effects of photo-induced graft polymerization of
47
48 2-methacryloyloxyethyl phosphorylcholine on physical properties of cross-linked polyethylene
49
50 in artificial hip joints. *J Mater Sci Mater Med* 2007;18:1809–1815.
51
52
53
54
55
56 22. Ishihara K, Ueda T, Nakabayashi N. Preparation of phospholipid polymers and their properties
57
58 as polymer hydrogel membranes. *Polym J* 1990;22(5):355–360.
59
60
23. Ishihara K, Ziats NP, Tierney BP, Nakabayashi N, Anderson JM. Protein adsorption from

- 1
2
3 human plasma is reduced on phospholipids polymers. *J Biomed Mater Res*
4
5
6 1991;25(11):1397–1407.
7
8
9 24. Goda T, Konno T, Takai M, Moro T, Ishihara K. Biomimetic phosphorylcholine polymer
10
11 grafting from polydimethylsiloxane surface using photo-induced polymerization. *Biomaterials*
12
13 2006;27(30):5151–5160.
14
15
16
17
18 25. Sibarani J, Takai M, Ishihara K. Surface modification on microfluidic devices with
19
20 2-methacryloyloxyethyl phosphorylcholine polymers for reducing unfavorable protein
21
22 adsorption. *Colloids Surf B Biointerfaces* 2007;54(1):88–93.
23
24
25
26
27
28 26. Ueda H, Watanabe J, Konno T, Takai M, Saito A, Ishihara K. Asymmetrically functional
29
30 surface properties on biocompatible phospholipid polymer membrane for bioartificial kidney. *J*
31
32 *Biomed Mater Res A*. 2006;77(1):19–27.
33
34
35
36
37 27. Palmer RR, Lewis AL, Kirkwood LC, Rose SF, Lloyd AW, Vick TA, Stratford PW. Biological
38
39 evaluation and drug delivery application of cationically modified phospholipid polymers.
40
41 *Biomaterials* 2004;25:4785–4796.
42
43
44
45
46
47 28. Snyder TA, Tsukui H, Kihara S, Akimoto T, Litwak KN, Kameneva MV, Yamazaki K, Wagner
48
49 WR. Preclinical biocompatibility assessment of the EVAHEART ventricular assist device:
50
51 Coating comparison and platelet activation. *J Biomed Mater Res A*. 2007;81(1):85–92.
52
53
54
55
56 29. Kuiper KJ, Nordrehaug JE. Early mobilization after protamine reversal of heparin following
57
58 implantation of phosphorylcholine-coated stents in totally occluded coronary arteries. *Am J*
59
60 *Cardiol* 2000;85:698–702.

- 1
2
3
4
5
6
7
8
9
10
11
12
13
14
15
16
17
18
19
20
21
22
23
24
25
26
27
28
29
30
31
32
33
34
35
36
37
38
39
40
41
42
43
44
45
46
47
48
49
50
51
52
53
54
55
56
57
58
59
60
30. Galli M, Sommariva L, Prati F, Zerboni S, Politi A, Bonatti R, Mameli S, Butti E, Pagano A, Ferrari G. Acute and mid-term results of phosphorylcholine-coated stents in primary coronary stenting for acute myocardial infarction. *Cathet Cardiovasc Intervent* 2001;53:182–187.
 31. Lewis AL, Hughes PD, Kirkwood LC, Leppard SW, Redman RP, Tolhurst LA, Stratford PW. Synthesis and characterisation of phosphorylcholine-based polymers useful for coating blood filtration devices. *Biomaterials* 2000;21:1847–1859.
 32. Pavoov PV, Gearing BP, Muratoglu O, Cohen RE, Bellare A. Wear reduction of orthopaedic bearing surfaces using polyelectrolyte multilayer nanocoatings. *Biomaterials* 2006;27:1527–1533.
 33. Yamamoto M, Kato K, Ikada Y. Ultrastructure of the interface between cultured osteoblasts and surface-modified polymer substrates. *J Biomed Mater Res* 1997;37:29–36.
 34. Wang P, Tan KL, Kang ET. Surface modification of poly(tetrafluoroethylene) films via grafting of poly(ethylene glycol) for reduction in protein adsorption. *J Biomater Sci Polym Ed* 2000;11:169–186.
 35. Iwata R, Suk-In P, Hoven VP, Takahara A, Akiyoshi K, Iwasaki Y. Control of nanobiointerfaces generated from well-defined biomimetic polymer brushes for protein and cell manipulations. *Biomacromolecules* 2004;5:2308–2314.
 36. Yoshida K, Greener EH. Effects of coupling agents on mechanical properties of metal oxide-polymethacrylate composites. *J Dent* 1994;22:57–62.
 37. Matinlinna JP, Vallittu PK. Bonding of resin composites to etchable ceramic surfaces - an

- 1
2
3 insight review of the chemical aspects on surface conditioning. *J Oral Rehabil*
4
5
6 2007;34(8):622–630.
- 7
8
9 38. Bryant SJ, Nuttelman CR, Anseth KS. Cytocompatibility of UV and visible light
10
11 photoinitiating systems on cultured NIH/3T3 fibroblasts in vitro. *J Biomater Sci Polym Ed.*
12
13 2000;11(5):439–457.
- 14
15
16
17
18 39. ASTM F75-01: Standard specification for cobalt-28 chromium-6 molybdenum alloy casting
19
20 and casting alloy for surgical implants (UNS R30075). In: *Annual Book of ASTM Standards*
21
22 13, 2004.
- 23
24
25
26
27
28 40. ASTM F86-04: Standard practice for surface preparation and marking of metallic surgical
29
30 implants. In: *Annual Book of ASTM Standards* 13, 2004.
- 31
32
33
34 41. Kyomoto M, Iwasaki Y, Moro T, Konno T, Miyaji F, Kawaguchi H, Takatori Y, Nakamura K,
35
36 Ishihara K. High lubricious surface of cobalt-chromium-molybdenum alloy prepared by
37
38 grafting poly(2-methacryloyloxyethyl phosphorylcholine). *Biomaterials*
39
40 2007;28(20):3121–3130.
- 41
42
43
44
45
46
47 42. Seo M, Sato N. Differential composition profiles in depth of thin anodic oxide films on
48
49 iron-chromium alloy. *Surface Science* 1979;86:601–609.
- 50
51
52
53 43. Ishihara K, Iwasaki Y, Ebihara S, Shindo Y, Nakabayashi N. Photoinduced graft polymerization
54
55 of 2-methacryloyloxyethyl phosphorylcholine on polyethylene membrane surface for obtaining
56
57 blood cell adhesion resistance. *Colloids Surf B Biointerfaces* 2000;18(3-4):325–335.
- 58
59
60
61 44. Kyomoto M, Moro T, Konno T, Takadama H, Yamawaki N, Kawaguchi H, Takatori Y,

- 1
2
3 Nakamura K, Ishihara K. Enhanced wear resistance of modified cross-linked polyethylene by
4
5 grafting with poly(2-methacryloyloxyethyl phosphorylcholine). *J Biomed Mater Res A*
6
7
8
9 2007;82(1):10–17.
- 10
11
12 45. Kyomoto M, Moro T, Miyaji F, Hashimoto M, Kawaguchi H, Takatori Y, Nakamura K,
13
14
15 Ishihara K. Effect of 2-methacryloyloxyethyl phosphorylcholine concentration on
16
17
18 photo-induced graft polymerization of polyethylene in reducing the wear of orthopaedic
19
20
21 bearing surface. *J Biomed Mater Res A*, in press.
- 22
23
24 46. Northwood E, Fisher J. A multi-directional in vitro investigation into friction, damage and wear
25
26
27
28 of innovative chondroplasty materials against articular cartilage. *Clinical Biomechanics*,
29
30
31 2007;22(7):834–842.
- 32
33
34 47. ISO. Plastics–Film and sheeting–Measurement of water-contact angle of
35
36
37 corona-treated films. 2004. International Organization for Standardization 15989.
- 38
39
40 48. ASTM F732-00: Standard test method for wear testing of polymeric materials used in total
41
42
43 joint prostheses. In: *Annual Book of ASTM Standards* 13, 2004.
- 44
45
46 49. Li YS, Tran T, Xu Y, Vecchio NE. Spectroscopic studies of trimethoxypropylsilane and
47
48
49 bis(trimethoxysilyl)ethane sol–gel coatings on aluminum and copper. *Spectrochimica Acta Part*
50
51
52 *A: Molecular and Biomolecular Spectroscopy* 2006;65(3–4):779–786.
- 53
54
55 50. Puleo DA. Biochemical surface modification of Co-Cr-Mo. *Biomaterials* 1996;17(2):217–222.
- 56
57
58 51. Matsuda T, Kaneko M, Ge S. Quasi-living surface graft polymerization with phosphorylcholine
59
60 group(s) at the terminal end. *Biomaterials* 2003;24:4507–4515.

- 1
2
3 52. Braunecker WA, Matyjaszewski K. Controlled/living radical polymerization: Features,
4
5 developments, and perspectives. *Progress in Polymer Science* 2007;32(1):93-146.
6
7
- 8
9 53. Saldívar-García AJ, Lopez HF. Microstructural effects on the wear resistance of wrought and
10
11 as-cast Co-Cr-Mo-C implant alloys. *J Biomed Mater Res A*. 2005;74(2):269–274.
12
13
- 14
15 54. Sheeja D, Tay BK, Nung LN. Tribological characterization of surface modified UHMWPE
16
17 against DLC-coated Co–Cr–Mo. *Surf Coat Technol* 2005;190(2-3):231–237.
18
19
- 20
21 55. Saikko V. Wear and friction properties of prosthetic joint materials evaluated on a reciprocating
22
23 pin-on-flat apparatus. *Wear* 1993;166(2):169–178.
24
25
- 26
27 56. Ishikawa Y, Hiratsuka K, Sasada T. Role of water in the lubrication of hydrogel. *Wear*
28
29 2006;261:500–504.
30
31
- 32
33 57. Ho SP, Nakabayashi N, Iwasaki Y, Boland T, LaBerge M. Frictional properties of
34
35 poly(MPC-co-BMA) phospholipid polymer for catheter applications. *Biomaterials*
36
37 2003;24(28):5121–5129.
38
39
- 40
41 58. Naka MH, Morita Y, Ikeuchi K. Influence of proteoglycan contents and of tissue hydration on
42
43 the frictional characteristics of articular cartilage. *Proc Inst Mech Eng [H]*.
44
45 2005;219(3):175–182.
46
47
- 48
49 59. Bell CJ, Ingham E, Fisher J. Influence of hyaluronic acid on the time-dependent friction
50
51 response of articular cartilage under different conditions. *Proc Inst Mech Eng [H]*
52
53 2006;220(1):23–31.
54
55
- 56
57 60. Kobayashi M, Terayama Y, Hosaka N, Kaido M, Suzuki A, Yamada N, Torikai N, Ishihara K,
58
59
60

1
2
3 Takahara A. Friction behavior of high-density poly(2-methacryloyloxyethyl
4
5 phosphorylcholine) brush in aqueous media. *Soft Matter* 2007;2:740–746.
6
7

8
9 61. Yamamoto S, Ejaz M, Tsujii Y, Fukuda T. Surface interaction forces of well-defined,
10
11 high-density polymer brushes studied by atomic force microscopy. 2. Effect of graft density.
12
13

14
15 *Macromolecules* 2000;33(15):5608–5612.
16
17

18
19 62. Raviv U, Glasson S, Kampf N, Gohy JF, Jérôme R, Klein J. Lubrication by charged polymers.
20
21

22
23 *Nature* 2003;425:163–165.
24
25
26
27
28
29
30
31
32
33
34
35
36
37
38
39
40
41
42
43
44
45
46
47
48
49
50
51
52
53
54
55
56
57
58
59
60

Figure captions

TABLE I Chemical composition (%) of the Co-Cr-Mo alloy

TABLE II Coefficients of dynamic friction of various bearing couples in previous studies

Figure 1. Chemical reaction on Co-Cr-Mo during polymerization of MPC.

Figure 2. FT-IR/ATR spectra of untreated Co-Cr-Mo and Co-Cr-Mo-g-MPC surfaces with a 0.50-mol/L MPC concentration and a 90-min photoirradiation time.

Figure 3. Surface elemental concentrations in the Co-Cr-Mo-g-MPC surface as a function of the photoirradiation time for various MPC concentrations in feeds. Bar: standard deviations.

Figure 4. Static-water contact angle of the Co-Cr-Mo-g-MPC surface as a function of the photoirradiation time for various MPC concentrations in feeds. Bar: standard deviations.

Figure 5. Cross-sectional TEM images of the Co-Cr-Mo-g-MPC surface with various MPC concentration in feeds and a 90-min photoirradiation time. Aluminum coating layers

1
2
3 (approximately 70 nm) for preparation of TEM observation specimen are shown above
4
5
6 the poly(MPC) layer of the Co-Cr-Mo-g-MPC surface. In (a) and (c), small
7
8
9 open-circles (P1–5) indicate EDX analysis points. Bar: 200 nm.
10

11
12
13
14
15 Figure 6. EDX spectra of the Co-Cr-Mo-g-MPC surface with a 0.5-mol/L MPC concentration
16
17
18 and a 90-min photoirradiation time. The spectra were analyzed on the cross-section
19
20
21 (P1–5) of the untreated Co-Cr-Mo and Co-Cr-Mo-g-MPC in Fig. 5.
22

23
24
25
26
27
28 Figure 7. Coefficients of dynamic friction for the various types of pins sliding against the
29
30
31 untreated Co-Cr-Mo and Co-Cr-Mo-g-MPC plates. Bar: standard deviations.
32

33
34
35
36
37 Figure 8. Images of high-density grafted poly(MPC)/low-density grafted poly(MPC) and
38
39
40 high-density grafted poly(MPC)/high-density grafted poly(MPC) bearing interfaces.
41
42
43
44
45
46
47
48
49
50
51
52
53
54
55
56
57
58
59
60

TABLE I Chemical composition (%) of the o-Cr-Mo alloy

Cr	Mo	C	Ni	Fe	Si	Mn	Al	Co
28.54	6.07	0.01	0.02	0.05	0.40	0.31	0.02	Bal.

For Peer Review

TABLE II Coefficients of dynamic friction of various bearing couples in previous studies

Bearing couple		Friction coefficient	Reference
Pin	Disc or plate		
Co-Cr-Mo	Co-Cr-Mo	0.19 – 0.27	41, 53
UHMWPE	Co-Cr-Mo	0.05 – 0.13	41, 54, 55
CLPE-g-MPC	MPC “grafted to” Co-Cr-Mo	0.07 – 0.13	41
Cartilage	Stainless steel	0.01 – 0.05	58
Cartilage	Cartilage	0.02	59

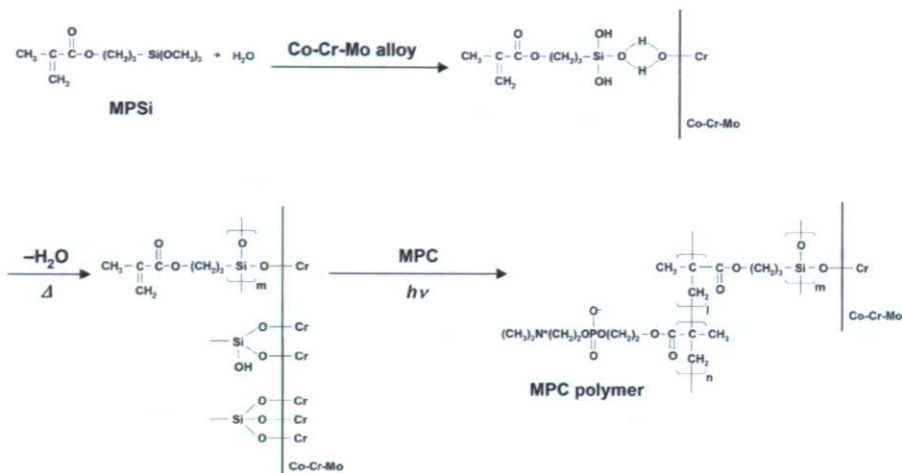


Figure 1. Chemical reaction on Co-Cr-Mo during polymerization of MPC.
61x34mm (600 x 600 DPI)

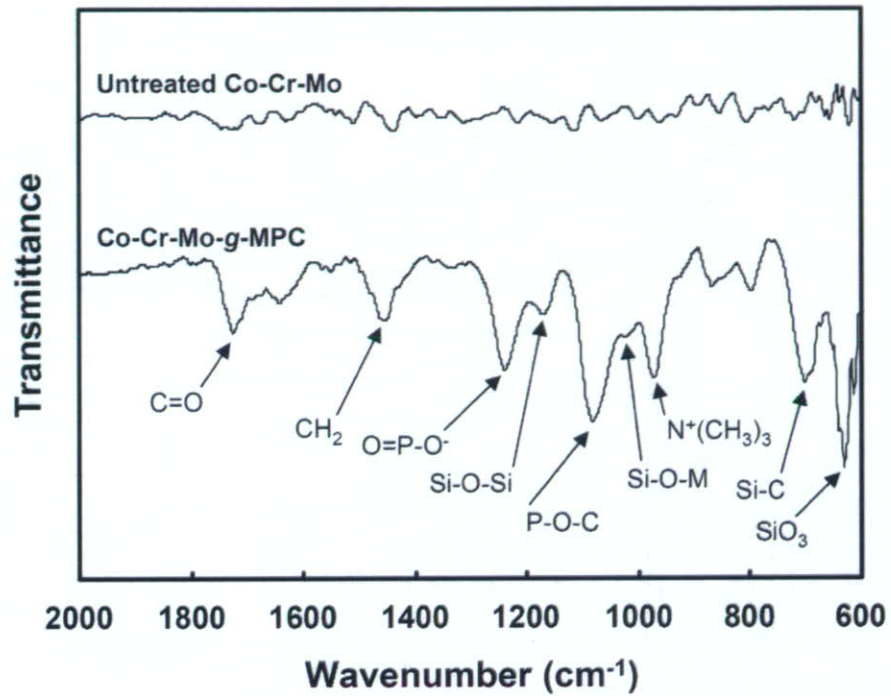


Figure 2. FT-IR/ATR spectra of untreated Co-Cr-Mo and Co-Cr-Mo-g-MPC surfaces with a 0.50-mol/L MPC concentration and a 90-min photoirradiation time.
61x49mm (600 x 600 DPI)

1
2
3
4
5
6
7
8
9
10
11
12
13
14
15
16
17
18
19
20
21
22
23
24
25
26
27
28
29
30
31
32
33
34
35
36
37
38
39
40
41
42
43
44
45
46
47
48
49
50
51
52
53
54
55
56
57
58
59
60

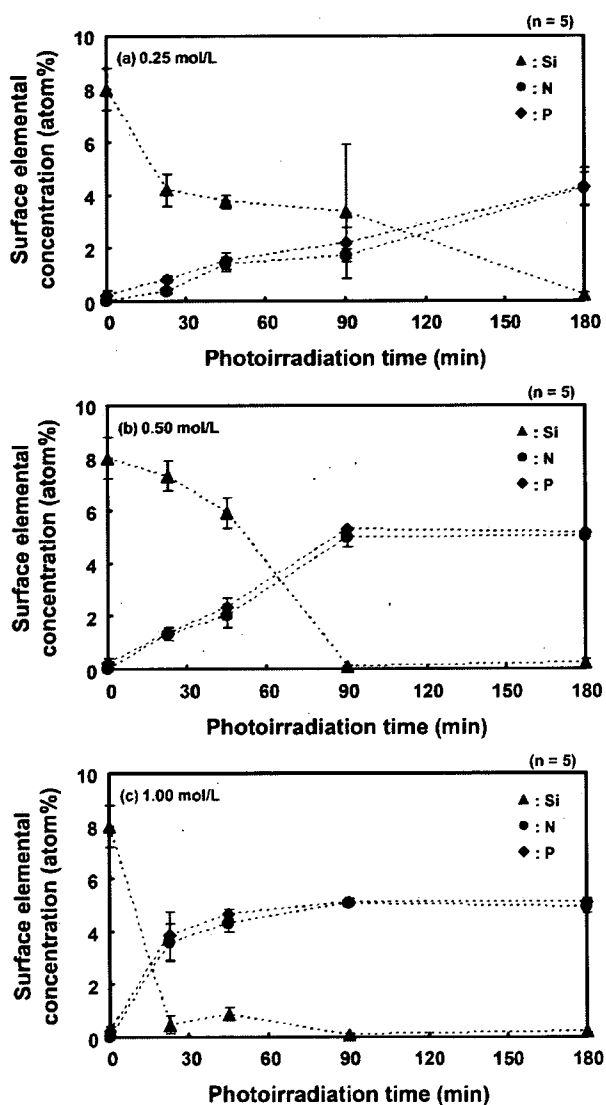


Figure 3. Surface elemental concentrations in the Co-Cr-Mo-g-MPC surface as a function of the photoirradiation time for various MPC concentrations in feeds. Bar: standard deviations.

152x272mm (600 x 600 DPI)

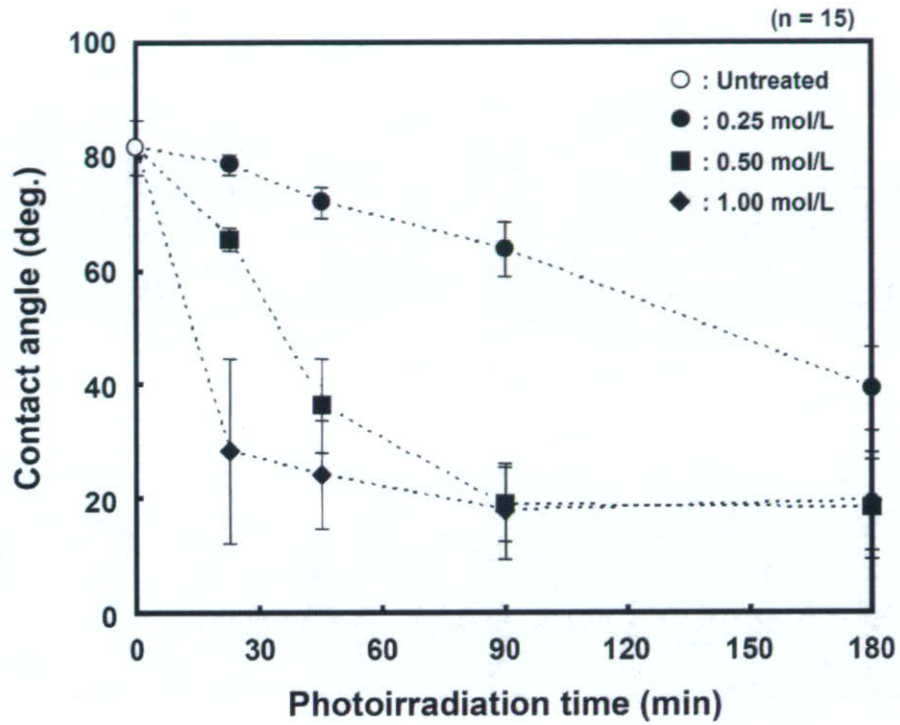


Figure 4. Static-water contact angle of the Co-Cr-Mo-g-MPC surface as a function of the photoirradiation time for various MPC concentrations in feeds. Bar: standard deviations. 66x53mm (600 x 600 DPI)

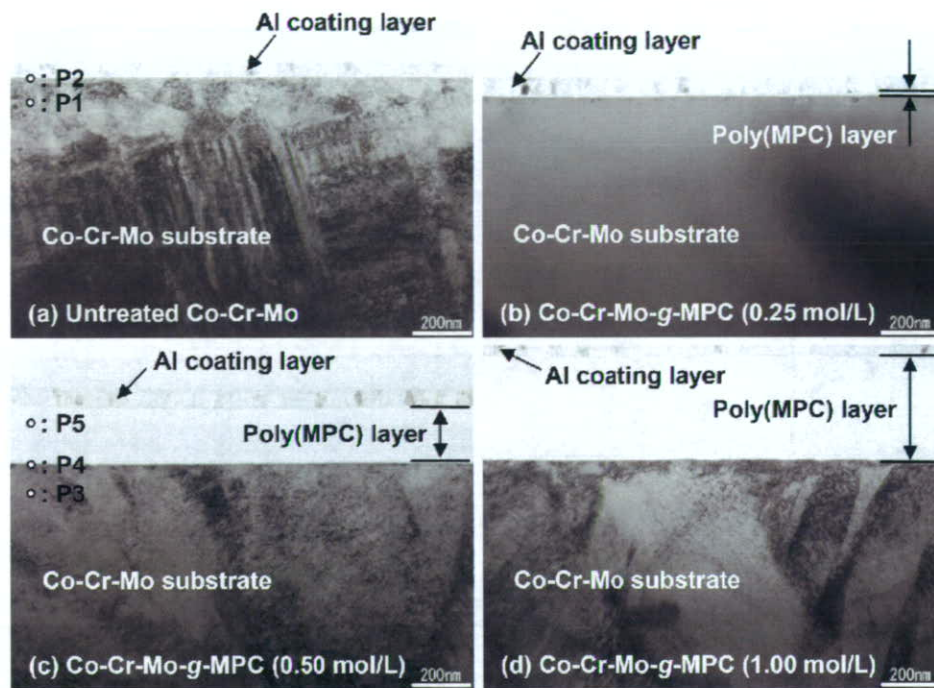


Figure 5. Cross-sectional TEM images of the Co-Cr-Mo-g-MPC surface with various MPC concentration in feeds and a 90-min photoirradiation time. Aluminum coating layers (approximately 70 nm) for preparation of TEM observation specimen are shown above the poly(MPC) layer of the Co-Cr-Mo-g-MPC surface. In (a) and (c), small open-circles (P1–5) indicate EDX analysis points. Bar: 200 nm.

82x62mm (600 x 600 DPI)

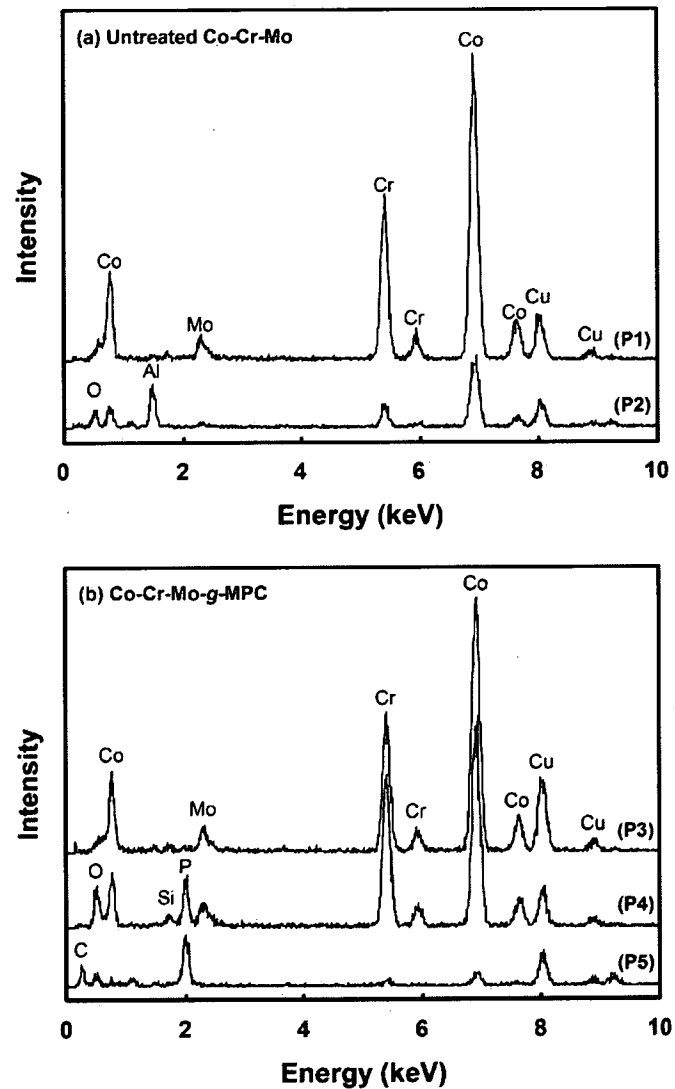


Figure 6. EDX spectra of the Co-Cr-Mo-g-MPC surface with a 0.5-mol/L MPC concentration and a 90-min photoirradiation time. The spectra were analyzed on the cross-section (P1-5) of the untreated Co-Cr-Mo and Co-Cr-Mo-g-MPC in Fig. 5.

123x194mm (600 x 600 DPI)

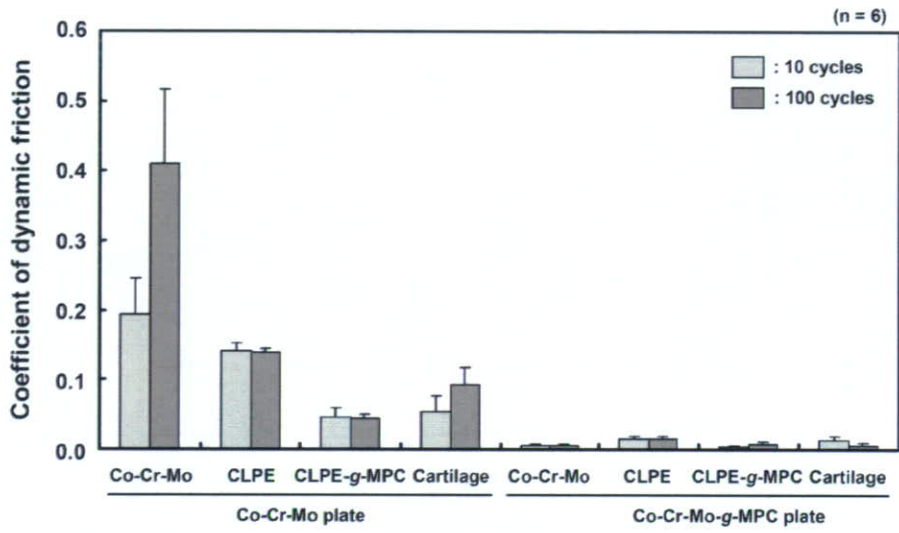


Figure 7. Coefficients of dynamic friction for the various types of pins sliding against the untreated Co-Cr-Mo and Co-Cr-Mo-g-MPC plates. Bar: standard deviations.
65x37mm (600 x 600 DPI)

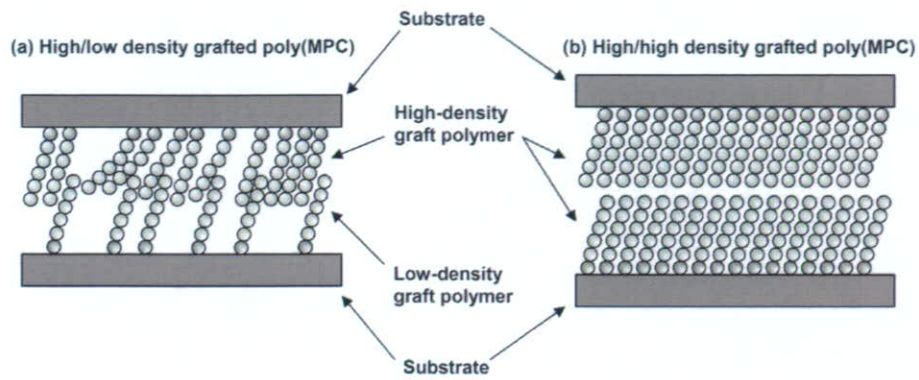


Figure 8. Images of high-density grafted poly(MPC)/low-density grafted poly(MPC) and high-density grafted poly(MPC)/high-density grafted poly(MPC) bearing interfaces.
45x19mm (600 x 600 DPI)

ポリエチレンライナー表面の MPC 処理は 人工股関節の弛みを抑制する ——ナノ表面制御による長寿命型人工股関節の開発——

東京大学医学部整形外科

茂呂 徹・高取 吉雄・中村 耕三

川口 浩

東京大学大学院工学系研究科

石原 一彦

はじめに

人工股関節手術後に生じる弛み (loosening) はその長期予後を決する重大かつ深刻な合併症である¹⁾。弛みは、人工股関節摺動面から生じる超高分子量ポリエチレン (ultra high molecular weight polyethylene: PE) の摩耗粉をマクロファージ (MΦ) が貪食して惹起される人工股関節周囲の骨吸収が主因である。摩耗粉を貪食した MΦ はサイトカ

インやプロスタグランジン (PG) を分泌する。これらの生体活性物質は破骨細胞分化因子・receptor activator of NF-κB ligand (RANKL) の発現を誘導し、その結果破骨細胞の形成・活性化が促進され、人工股関節周囲の骨吸収に至る²⁾。したがって、弛みの抑制を目指した研究は、摩耗粉を減少させること、あるいは骨吸収を抑制すること、の2つの方向性で検討されてきたが、現在までに決定的な解決策は得られていない。

我々は、摩耗粉の産生を抑制し、かつ摩耗粉による骨吸収の誘導を阻止すればこの問題を解決できると考えた。生体の関節軟骨表面にはナノスケールのリン脂質層が存在し潤滑機構の改善に寄与している³⁾。そこで、生体適合性リン脂質ポリマー・2-methacryloyloxyethyl phosphorylcholine (MPC) ポリマーを PE ライナー表面にナノスケールで光学的にグラフトする方法 (MPC ポリマー処理) を創案した (図1)。この処理は、紫外線を用いて MPC と PE の炭素原子同士に強力かつ安定な共有結合をさせるもので、表層のみの処理であり、基材である PE 自体には影響を及ぼさない⁴⁾。我々は、本技術の臨床応用を目指し、耐摩耗性と摩耗粉が骨吸収に及ぼす影響の観点から関節摺動面の MPC ポリマー

Grafting of biocompatible MPC polymer on the polyethylene liner for preventing loosening and improving longevity of the artificial hip joint

Department of Orthopaedic Surgery,
Faculty of Medicine, The University of Tokyo
Toru Moro et al.

Key words : 人工股関節全置換術 (total hip arthroplasty)
弛み (aseptic loosening)
オステオライシス (osteolysis)